Roles of Physiological and Nonphysiological Information in Sun-Induced Chlorophyll Fluorescence Variations for Detecting Cotton Verticillium Wilt

Junru Zhou, Changping Huang, Yaohui Gui, Mi Yang, Ze Zhang, Wenjiang Huang, Lifu Zhang, *Senior Member, IEEE*, and Qingxi Tong

***Abstract*—Sun-induced chlorophyll fluorescence (SIF) has been a promising indicator of plants' physiological status, but its response to physiological changes under the verticillium wilt (VW) stress of cotton plants is complicated by concurrent nonphysiological changes. The relative contributions of the above two components to SIF variations are unclear at different VW stress severities, hindering the accurate diagnosis of VW levels. Therefore, the objective of this study is to investigate the dynamic responses of SIF, physiological and nonphysiological factors, and to evaluate the contributions of the two factors to SIF variations under different VW stress degrees of cotton. We continuously observed the diurnal variation of the top-of-canopy reflectance and SIF on healthy and VW-infected cotton during the peak incidence period of VW disease. To accurately quantify the relative contribution of each component to SIF, we proposed a practical strategy to estimate unmeasurable parameter when using Lindeman, Merenda, and Gold method. The results demonstrated the dominant role of physiological factors in SIF with an arch diurnal change pattern at the early stages of VW development. As the VW severity increased, the contribution of physiological components declined, with the maximum contribution decreasing by 47.7%, and the diurnal pattern was disrupted, with the diurnal variation amplitude of the parameter declining by 63.4%, followed by a shift in the regulatory role toward nonphysiological factors. This study contributes to a further understanding of the roles of physiological and nonphysiological components in SIF variations of cotton under VW stress, thus advancing the accurate monitoring of VW stress severity.**

***Index Terms*—Cotton verticillium wilt (VW), nonphysiological, photosynthesis, sun-induced chlorophyll fluorescence (SIF).**

I. Introduction

COTTON is an important cash crop and natural fiber supply source in the world. Verticillium Wilt (VW) is the most common and devastating disease occurring in the growth and maturation of cotton [1], [2]. The *Verticillium dahliae* that causes VW first invades the root surface of cotton in the soil [3], and then the vascular tissue, finally accumulates and expands in the cotton plant blocking the transport of water and nutrition. This obstruction caused a decrease in photosynthesis, the browning of vascular bundle, and the yellow wilting of cotton leaves.

Under VW stress, the morphology and physiological state of cotton undergoes changes, resulting in alterations in some characteristic bands of the spectrum compared with healthy plants. Previous studies have used remote sensing technology to extract spectral characteristics at both leaf [4], [5], [6] and canopy [7], [8], [9], [10], [11] scales, aiming to monitor the impact of VW on cotton plants and to determine the degree of VW stress. Disease monitoring based on reflectance spectral characteristics relies on spectral responses to variations in physiological, biochemical, and canopy structure indicators, such as vegetation chlorophyll content, leaf water content, and leaf area index [12]. However, the above indicators do not change significantly until the plant has been stressed for a period, which cannot reflect the stressed state of vegetation timely at an early stage [13]. Compared with reflectance spectra, chlorophyll fluorescence spectra can reflect physiological changes earlier and more sensitively [14], [15], [16], [17].

Sun-induced chlorophyll fluorescence (SIF) is a signal emitted by plant chlorophyll molecules in the range of 650–800 nm

Manuscript received 9 January 2024; revised 26 February 2024; accepted 4 April 2024. Date of publication 18 April 2024; date of current version 29 April 2024. This work was supported in part by the Key Research Program of Frontier Sciences, CAS, under Grant ZDBS-LY-DQC012, in part by the National Natural Science Foundation of China under Grant 41971321 and Grant 42201392, and in part by the Science and Technology Major Program of BINGTUAN under Grant 2023AA008. The work of Changping Huang was supported by Youth Innovation Promotion Association, CAS, under Grant Y2021047. *(Corresponding author: Changping Huang.)*

Junru Zhou, Changping Huang, and Yaohui Gui are with the National Engineering Laboratory for Satellite Remote Sensing Applications, Aerospace Information Research Institute, Chinese Academy of Sciences, Beijing 100094, China, and also with the University of Chinese Academy of Sciences, Beijing 100049, China (e-mail: zhoujunru21@mails.ucas.ac.cn; huangcp@aircas.ac.cn; guiyaohui22@mails.ucas.ac.cn).

Mi Yang and Ze Zhang are with the Xinjiang Production and Construction Crop Oasis Eco-Agriculture Key Laboratory, College of Agriculture, Shihezi University, Shihezi 832003, China (e-mail: yangmi@stu.shzu.edu.cn; zhangze1227@shzu.edu.cn).

Wenjiang Huang is with the State Key Laboratory of Remote Sensing Science, Aerospace Information Research Institute, Chinese Academy of Sciences, Beijing 100094, China, and also with the College of Resources and Environment, University of Chinese Academy of Sciences, Beijing 100049, China (e-mail: huangwj@aircas.ac.cn).

Lifu Zhang and Qingxi Tong are with the National Engineering Laboratory for Satellite Remote Sensing Applications, Aerospace Information Research Institute, Chinese Academy of Sciences, Beijing 100094, China (e-mail: zhanglf@aircas.ac.cn; tqxi@263.net).

Digital Object Identifier 10.1109/JSTARS.2024.3390546

under natural sunlight. SIF is closely related to plant photosynthesis, and previous studies have demonstrated its potential to detect the state of vegetation under environmental stress quickly [18]. Some researchers have used SIF to monitor the response of vegetation under stress, such as disease stress [7], [8], [19] and water stress [20], [21], [22]. As a byproduct of electron re-excitation during the process of photosynthesis, SIF is first transmitted from the photosystem to the leaf surface, then interacts with the canopy leaves (reflection, scattering, and absorption) before escaping the canopy, and finally reaches the sensor. The complex process of radiation transmission makes the canopy SIF signal not only contain the information on plant photosynthetic physiology but also is affected by changes in canopy structure [23], [24], [25]. According to the light-use-efficient concept model of gross primary production (GPP) [26], the SIF conceptualization formula [18] is shown as follows:

$$\mathrm{SIF} = \mathrm{PAR} \times \mathrm{fPAR} \times \Phi F \times f_{\mathrm{esc}}. \tag{1}$$

The canopy SIF observed by the sensor consists of four factors, the photosynthetically active radiation (PAR), the fraction of the PAR absorbed by the vegetation (fPAR), the fraction of all emitted SIF photons escapes the canopy (f_{esc}), and the physiological SIF emission efficiency at the canopy level (ΦF). Among them, PAR, fPAR, and f_{esc} are usually used to characterize nonphysiological information, and ΦF is used to characterize physiological state of leaves [25]. When the sensor detects the change in SIF, it is actually the composite result of multiple factors.

Previous studies have employed active chlorophyll fluorescence to monitor the effect of VW at the leaf scale [5], [27]. Chlorophyll fluorescence at the leaf level characterizes the physiological status of individual leaves, and the physiological status of leaves at different positions on the same plant varies. Therefore, solely relying on leaf-level fluorescence is challenging to accurately reflect the degree of stress experienced by the entire vegetation. Fluorescence at the canopy level is needed to reflect the stress status of the vegetation. However, the observed SIF at the canopy scale is also influenced by the canopy structure. The presence of VW in cotton plants induces changes in both photosynthetic physiology and canopy structure. Both of these alterations may lead to a reduction in SIF at the canopy scale. Identifying the primary factor driving this reduction would facilitate the differentiation of cotton plants under VW stress from healthy ones and contribute to the accurate monitoring of VW severity. Therefore, it is essential to understand the relative importance of each factor in influencing the change of SIF under the stress of VW at different levels in order to further understand the impact of VW stress on cotton.

The relative importance analysis method proposed by Lindeman, Merenda, and Gold (LMG) is employed to explore the contribution of a single regression to the change of the dependent variable [28]. This method effectively mitigates the influence of variable order in regression and accurately computes the relative importance of each independent variable concerning the dependent variable. Some scholars have used it to investigate the relative importance of factors in (1) to the change of SIF [29], [30]. The parameter ΦF in the SIF conceptual model, which cannot be measured directly, is usually derived through calculations involving SIF and other parameters in current research, as shown in (2). It is difficult to represent f_{esc} and fPAR individually; thus, former studies always using a spectral index to represent fPAR $\times$ f_{esc}, such as near-infrared reflectance of vegetation (NIRv). When calculating the relative importance of PAR, ΦF, and NIRv to SIF variations, using the same index to represent fPAR $\times$ f_{esc} and calculate ΦF results in ΦF being expressed linearly in terms of other parameters (SIF, PAR, and NIRv). This violates the model's requirement for the independent variables to be linearly independent. We found that introducing random errors could mask this conflict, creating the illusion of data that satisfies the requirements, thereby enabling the model to produce a result. This will introduce uncertainty into the results, as random errors may alter the relative importance of each independent variable. It is essential to propose a practical strategy for estimating ΦF that meets the model's requirements and assess the influence of random errors of the original estimating method

$$\Phi F = \frac{\mathrm{SIF}}{\mathrm{PAR} \times \mathrm{fPAR} \times f_{\mathrm{esc}}}. \tag{2}$$

This study aims to explore the effects of physiological and nonphysiological factors on the SIF of cotton under VW stress. We conducted continuous observation on seven cotton canopies and performed the following work:

1) explore the responses of nonphysiological factors, physiological factors, and SIF under different levels of VW stress;
2) quantify the contributions of physiological and nonphysiological information to SIF at different degrees of VW severity;
3) propose a practical strategy to estimate ΦF and quantify the impact of random errors on relative importance results.

II. Materials and Methods

A. Study Site

The study area is located in the VW disease field of the Shihezi Institute of Agricultural Sciences (44.33°N, 86.05°E) and the healthy field of the Agriculture College of Shihezi University (44.33°N, 86.06°E). In contrast to the healthy field, where the soil is free of *Verticillium dahliae*, the soil of the VW disease field is inoculated with the pathogen of VW before planting cotton each year. The two experimental fields have close distance and similar management measures, so they are good control subjects. Shihezi is located at the northern foot of Tianshan Mountain and the southern edge of Junger Basin. It has a temperate continental climate, with an average annual precipitation of 125–208 mm and an average annual temperature of 6.5–7.2 °C [10].

B. Field Measurements

Canopy scale spectrum and SIF diurnal variation data were obtained using an automated fluorescence observation system,

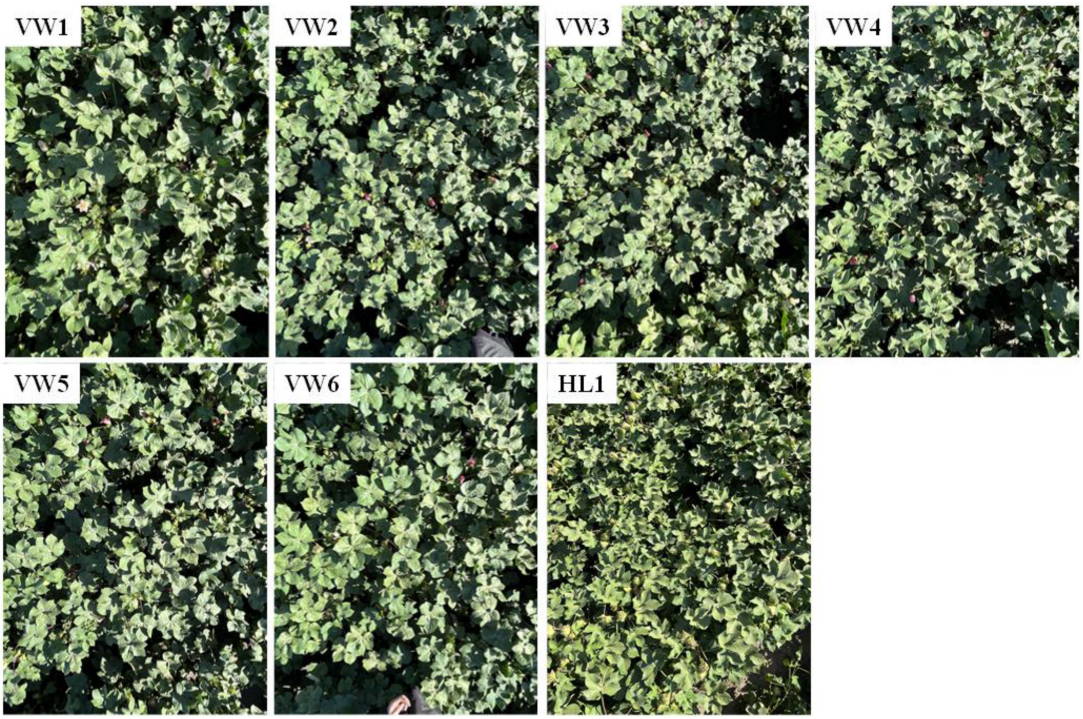

Fig. 1. Canopy observation points (VW1–VW6 are the six observation points in the disease field, and HL1 is the healthy points in the healthy field).

including a QE65 Pro spectrometer (Ocean Optics Inc., Dunedin, FL, USA). The QE65 Pro spectrometer has a band range of 640–800 nm, a spectral resolution of 0.39 nm, a spectral sampling interval of 0.15 nm, and a signal-to-noise ratio of 1000:1. The optical fiber used to measure the incident downwelling irradiance (E) is fitted with a cosine corrector, and the upwelling radiance (L) is measured through a bare optical fiber with a field-of-view of 25°.

From 26 July 2023 to 26 August 2023, long-term diurnal cotton canopy monitoring was conducted at six typical sites in the VW disease-affected fields (denoted as VW1–VW6) and at one typical site in the healthy field (denoted as HL1)(see Fig. 1). The probe for measuring E was installed on a straight rod and kept vertically upward at all times. The bare optical fiber for measuring L was installed on the instrument bracket to keep the probe always vertically downward to the canopy. Considering the width of the cotton plants in the field, the probe was positioned approximately 1.1 m above the top of the canopy. During the observation period, the daily observation time was from 10:00 to 18:00 (Beijing time) so as to prevent large errors in the measurement data when the solar altitude angle was too small.

In this study, the 3FLD (three bands FLD, 3FLD) algorithm proposed by Maier et al. [31] was used for SIF inversion, where $\lambda_{\text{in}} = 760.52$ nm, $\lambda_{\text{left}} = 758.05$ nm, and $\lambda_{\text{right}} = 768.03$ nm.

C. Parameter Calculation

We used near-infrared (R_{NIR}) and red (R_{red}) reflectance of plant canopy to calculate the normalized difference vegetation index (NDVI) and then the NIRv, which is widely used to approximate fPAR $\times f_{\text{esc}}$ [32]. We calculated NIRv using the canopy reflectance at 650–670 nm (red band, R_{red}) and 760–800 nm (near-infrared band, R_{NIR}). NIRv is expressed as follows [33]:

$$\text{NIRv} = \text{NDVI} \times R_{\text{NIR}} = \frac{R_{\text{NIR}} - R_{\text{red}}}{R_{\text{NIR}} + R_{\text{red}}} \times R_{\text{NIR}}. \quad (3)$$

The fluorescence correction vegetation index (FCVI) is an index developed for disentangling physiological and nonphysiological information infrared SIF [34]. In addition, the combined impacts of fPAR and f_{esc} can also be effectively approximated using FCVI. It was originally defined as the difference between near-infrared reflectance and broadband visible reflectance ranging from 400 to 700 nm ($R_{\overline{\text{vis}}}$)

$$\text{FCVI} = R_{\text{NIR}} - R_{\overline{\text{vis}}}. \quad (4)$$

Due to the limitation of the sensor band range, the reflectance of 650–700 nm is used to approximate the wideband visible light reflectance according to Yang et al. [35].

Canopy scale chlorophyll content was characterized by red edge NDVI (RENDVI) [36]

$$\text{RENDVI} = \frac{R_{\text{NIR}} - R_{\text{red edge}}}{R_{\text{NIR}} + R_{\text{red edge}}}. \quad (5)$$

In this study, no equipment could continuously observe PAR throughout the day, so the integration of incident radiation in the spectrum of 660–800 nm was used to approximate PAR, and the feasibility of this characterization method was also tested using actual measured PAR values. We denoted the integration of incident radiation in the spectrum of 660–800 nm as PAR_proxy and defined SIF_PAR = SIF/PAR_proxy.

It can be found from (1) that ΦF is a parameter that characterizes the physiological state of leaves, and PAR, fPAR, and f_{esc} represent the nonphysiological information, where PAR is photosynthetically active radiation, which is independent with the growth state of vegetation. Therefore, we separated PAR as an independent factor and combined fPAR and f_{esc} to represent the nonphysiological state of plant. In this study, we used NIRv and FCVI to approximate the characterization of fPAR $\times f_{\text{esc}}$ [32], [33], [34], then (1) convert into the following equation:

$$\begin{aligned} \text{SIF} &\approx \text{PAR} \times \Phi\text{F} \times \text{NIRv} \\ &\approx \text{PAR} \times \Phi\text{F} \times \text{FCVI}. \end{aligned} \tag{6}$$

According to (6), ΦF is calculated as follows:

$$\Phi F = \frac{\text{SIF}}{\text{PAR} \times \text{fPAR} \times f_{\text{esc}}} \approx \frac{\text{SIF}}{\text{PAR} \times \text{FCVI}}. \tag{7}$$

D. Relative Contributions of Physiological and Nonphysiological to SIF

This study used the LMG model [28] to analyze the relative importance of illumination (PAR), physiological (ΦF), and nonphysiological (fPAR $\times f_{\text{esc}}$) contributions to SIF changes. For variables with a linear relationship between the dependent and independent variables, the model can quantify the contribution of an independent variable to the change of dependent variable while considering the varying independent contributions of independent variables to dependent variables, as well as the different correlations between independent variables. The core idea of the LMG model is that R^2 represents the proportion of variance explained by a set of independent variables, different R^2 values are obtained by different combinations of independent variables, and finally the individual contribution of each independent variable to the change in the dependent variable is calculated. In this study, we first took the natural logarithm of (6) to make it into linear form, thus obtaining (8), and then used R language package *relaimpo* [37] to calculate the contribution of each independent variable to the dependent variable

$$\ln(\text{SIF}) = \ln(\text{PAR}) + \ln(\text{NIRv}) + \ln(\Phi F). \tag{8}$$

In relative importance analysis, we used NIRv to denote nonphysiological information, and when estimating ΦF, we employed FCVI to represent nonphysiological information according to (7).

As mentioned in Section I, adding random errors to input data enables the model to produce results. This study introduced 5 random error terms (see Table I) to 15 parallel samples, exploring their diverse impacts on the outcomes. To reduce the randomness of the experimental results, for the latter four types of Gaussian random noise in Table I, the experiment was repeated five times, and the average and variance of the relative changes were compared.

TABLE I
RANDOM ERRORS

Error name	Error type	Mean	Standard deviation
Round7	Round-off error		
GS_Std	Gaussian random noise	0	SIF standard deviation
GS_Std01	Gaussian random noise	0	0.1*SIF standard deviation
GS_001	Gaussian random noise	0	0.01
GS_005	Gaussian random noise	0	0.05

E. Data Preprocessing

Since the fluorescence automatic observation system used in the experiment works in a sequential measurement mode, it allows only one channel signal to be measured at a time using a single spectrometer. For each observation point, the E was measured (E_M), and then the L, with a 15–60 s delay in the measurement time. Under unstable weather conditions, rapid changes in the illumination occurred during the measurement, leading to notable differences between the real E when measuring L (E_L) and the measured E_M. It will result in a significant error in the calculation of canopy reflectance SIF derived from E and L, introducing uncertainty into the subsequent data analysis [38]. Therefore, before data processing, we filtered and removed abnormal data caused by abrupt changes in light intensity.

Cotton field disease outbreaks are influenced by the climatic conditions [39], especially temperature and humidity. The optimum temperature for the onset of VW of cotton is 22–28 °C, higher than 30 °C is not conducive to the onset, and more than 35 °C does not develop symptoms [40], [41], [42]. Meanwhile, the occurrence of VW of cotton is also related to humidity, and it is easy to develop when the relative humidity is suitable. Cotton flowering and boiling stage is during the summer in Xinjiang; most of the time, the temperature is high and the relative humidity is low, and the development of the disease is inhibited. When there is a sudden drop in temperature accompanied by rainfall, offering suitable conditions for disease onset, it is easy to cause a large area outbreak of VW. Based on the characteristics of cotton VW, the whole experimental period was divided into four subperiods ($T1$–$T4$) according to two temperature drop events and one regular irrigation event in the field. As shown in Fig. 2, $T1$–$T2$ and $T2$–T3 are divided by temperature drop events. $T3$–$T4$ is divided by a regular irrigation event since large-scale irrigation in a field will substantially change soil temperature, humidity, and near-surface microclimate. It was believed that the stress degree of cotton plants was prone to become more severe after each event. In this study, we used $T1|T2$ to represent the time period between $T1$ and $T2$, and similarly, this applies to other time periods.

III. RESULTS

Based on the development of VW stress in cotton plants throughout the entire experimental period, we categorized six VW observation points into three groups. VW1 represented a rapid intensification of VW stress during a certain subperiod, and VW2 and VW3 represented a gradual onset of disease

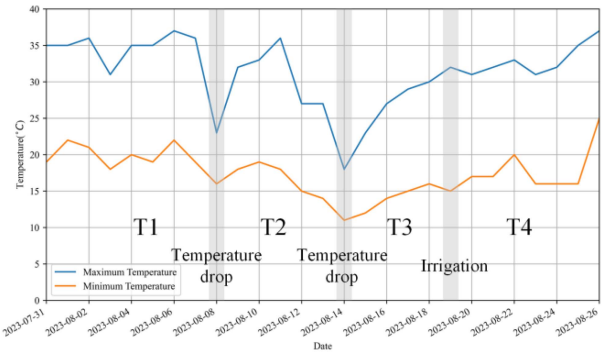

Fig. 2. Subperiod division during the experiment.

throughout the entire experimental period, culminating in a severe stress level; VW4, VW5, and VW6 represented a gradual onset of disease throughout the entire experimental period, resulting in a relatively lighter stress level. In the rest of this article, we will analyze the results using VW1, VW3, and VW4 as representatives, and the results for the rest VWs are shown in Appendix (see Figs. 9 and 10).

A. Responses of Vegetation Parameters to VW Stress

The changes of NIRv and FCVI, which represent the canopy structure characteristics, are shown in Fig. 3. The HL1canopy remained stable through all periods, whereas the canopy values of all VW observation points showed a downward trend with the increasing of VW severity. Several observation points, including VW3 and VW4, exhibited a gradual decline from $T1$ to $T4$, while specific observation points, such as VW1 during the $T2$ period, experienced a sudden plummet. As shown in Fig. 4, the VW1 canopy during $T2$ was much sparser than that during $T1$ due to the outbreak of VW of cotton plants in the canopy of VW1 region with the abrupt temperature drop of $T1|T2$. Based on the daily on-site investigation of cotton plants, the survey results indicate that during the $T1$ period, VW1 already exhibited mild symptoms of verticillium wilt. As VW1 had already been affected by verticillium wilt prior to the $T1|T2$ event, it was comparatively more vulnerable than the cotton plants at other observation points. Therefore, experiencing the same temperature drop event during $T1|T2$, VW1 would be more significantly affected and subsequent changes would be more pronounced. The RENDVI value of HL1 was stable in $T1$–$T3$ period, with a slight decline in $T4$ period. In contrast, the canopy exposed to VW stress had decreased before $T4$ period. VW1 exhibited a decline in the late $T2$ period, followed by a rebound in the $T3$ period and declined again in the $T4$ period. VW3 started to decline in the $T2$ period. VW4 remained relatively stable in the first two periods and began to decline in the $T3$ period.

Throughout the entire observation period (see Fig. 3), the SIF of all seven observed canopies, including HL1, showed a general declining trend, although with varying decline rates observed across different regions. The decline of SIF, following a period of initial stability, started at different times according to the varying onset times and degrees of VW stress. Among them, VW1 was relatively stable in $T1$ period, decreased in $T2$ period, and maintained its stability in $T3$ and $T4$ periods. The remaining VW observation points showed a slight decrease in $T1$ period, remained relatively stable in $T2$ period, and exhibited an obvious decreasing trend from $T3$ period. To eliminate the influence of PAR, we normalized SIF with PAR_proxy (SIF/PAR_proxy) as SIF_PAR, which exhibited a similar trend to SIF. The overall variation trend of ΦF, representing the physiological component of SIF, fluctuated and decreased at each observation point in different amplitudes. It also fluctuated between and within each subperiod.

B. Relative Importance of Individual Drivers to SIF Variations Under VW Stress

In Fig. 5, it can be found that the diurnal variation pattern of the relative importance of HL1 is consistent at each period of $T1$–$T4$. The diurnal variation pattern of the relative importance of PAR shows a "U" shape. The relative importance of ΦF exhibits an arch shape, which is lower in the morning and late afternoon, but higher near noon. The relative importance of NIRv is low and its variation is minimal. For observation points under VW stress, the pattern of variation for each factor in different periods was not as stable as HL1. In addition, the diurnal variation pattern of the relative importance of each parameter was found to be closely related to the degree of exposure to VW stress.

In the $T1$ period, the diurnal variation patterns of the VW1, VW3, and VW4 are similar to that of HL1. In the $T2$ period, the importance of ΦF for VW1 on SIF exhibited substantial variation, with its maximum values declined by 28.1%. Its diurnal variation pattern was destroyed, with higher values in the morning gradually decreasing until noon, increasing in the afternoon, followed by a subsequent decrease. Compared with $T1$ period, the importance of NIRv increased remarkably, with a maximum value increased by 358.7%, and displayed a diurnal variation pattern with an arch shape. It is noteworthy that its importance surpassed that of ΦF after 11 o'clock due to the pronounced intensification of VW stress of VW1 in the $T2$ period. The abrupt temperature drop during $T1|T2$ led to the outbreak of VW in cotton plants within the observation area of VW1, resulting in a significant alteration of the canopy structure from dense to sparse (see Fig. 4). In $T3$, the diurnal pattern of ΦF in VW1 partially recovered, although the value was low. Moreover, the importance of NIRv surpassed that of $T1$ and exceeded ΦF in the morning. The diurnal variation pattern of VW1 in $T4$ was similar to that in $T3$, and the importance of NIRv increased. The diurnal variation of VW3 parameters in $T2$ period was similar to that in $T1$ period, but it changed greatly in $T3$ period. The diurnal pattern of the importance of ΦF no longer presented an arch shape, instead, the importance within each time period in the morning is similar, as is the importance in the afternoon. The relative importance of NIRv increased compared with the previous two periods and exceeded ΦF in the afternoon. During $T4$, the relative importance of NIRv further increased compared with $T3$, exceeding ΦF at most times of the day. Meanwhile, the maximum value of ΦF decreased by 47.7%, and its diurnal variation amplitude declined by 63.4% compared with $T1$. The diurnal variation of the relative importance of VW4

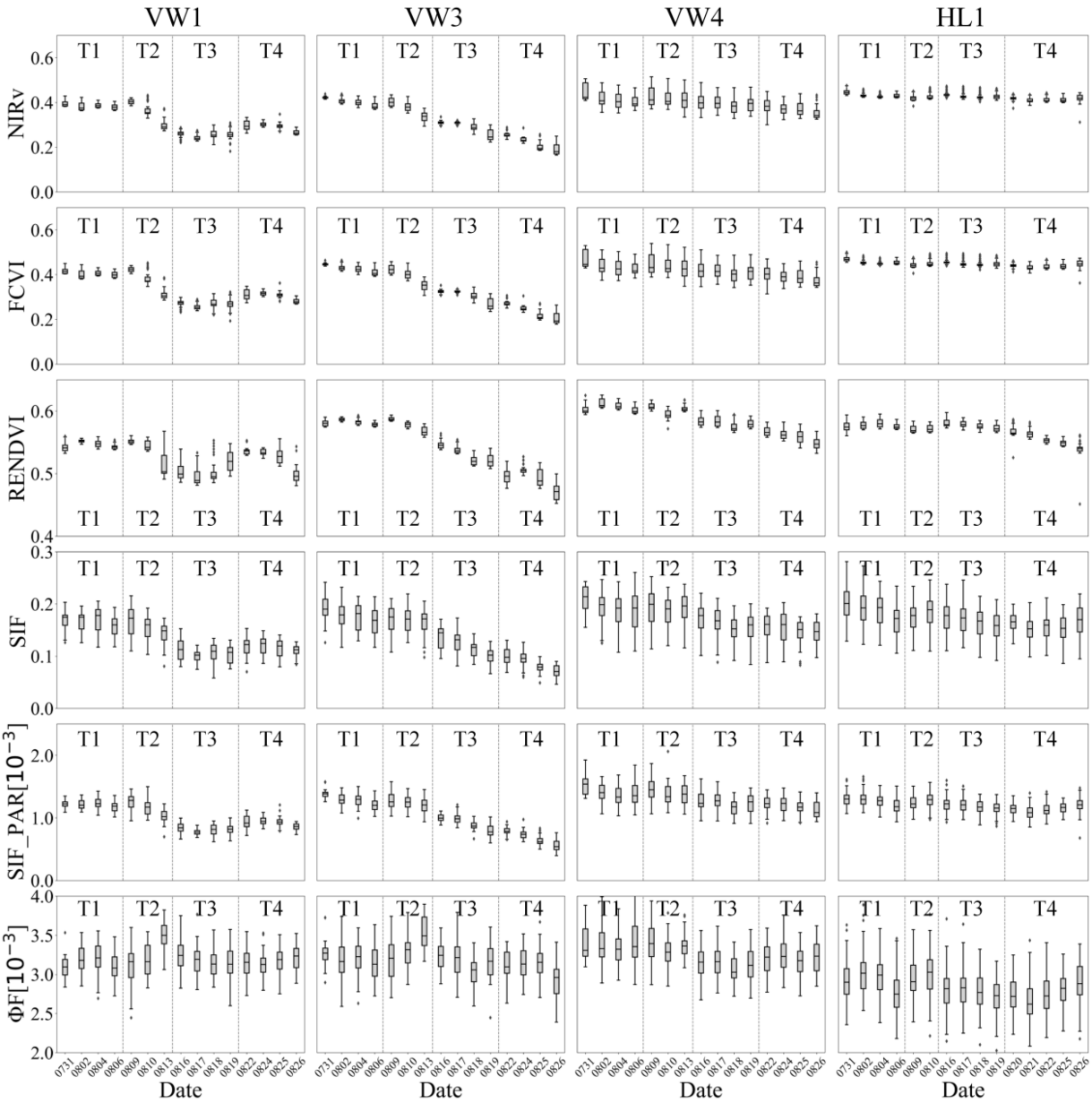

Fig. 3. Daily variations in nonphysiological factors (NIRv, FCVI, and RENDVI), SIF, SIF_PAR, and physiological factors (ΦF) during the experimental period. Each column represents VW1, VW3, VW4, and HL1.

parameters in $T2$ and $T3$ was similar to that in $T1$. In addition, the relative importance of ΦF in $T3$ experienced a slight decrease of 4.9%, yet it remained higher than other parameters. During $T4$, the relative importance of ΦF for VW4 decreased by 16.5% with a lower amplitude, declined by 3.7% compared with $T1$ period. The relative importance of NIRv became higher than PAR, but still lower than ΦF during midday.

In summary, at the early stages of VW development, SIF was mainly influenced by ΦF representing the photosynthetic physiological state of cotton. Its contribution increased in the morning, reached the maximum at noon, and then gradually decreased. Nonphysiological factor had a minor effect on SIF, with a limited range of change in a single day. As the VW stress intensified, the influence of ΦF on SIF decreased further, with the diurnal pattern destroyed, while the impact of NIRv increased, surpassing that of PAR but still lower than ΦF at noon. Under more severe VW stress, the contribution of ΦF on SIF was similar to that of NIRv, and its value remained stable throughout the day. NIRv increased further than before, was potentially higher than ΦF at noon, and even at most of the day under more severe stress.

C. Relative Change Induced by Random Error

Due to the limitations of the estimation method for ΦF in the existing studies, we used FCVI to calculate ΦF, which meets the requirement of the LMG model. In order to verify the capacity of NIRv and FCVI to represent the same physical meaning, and

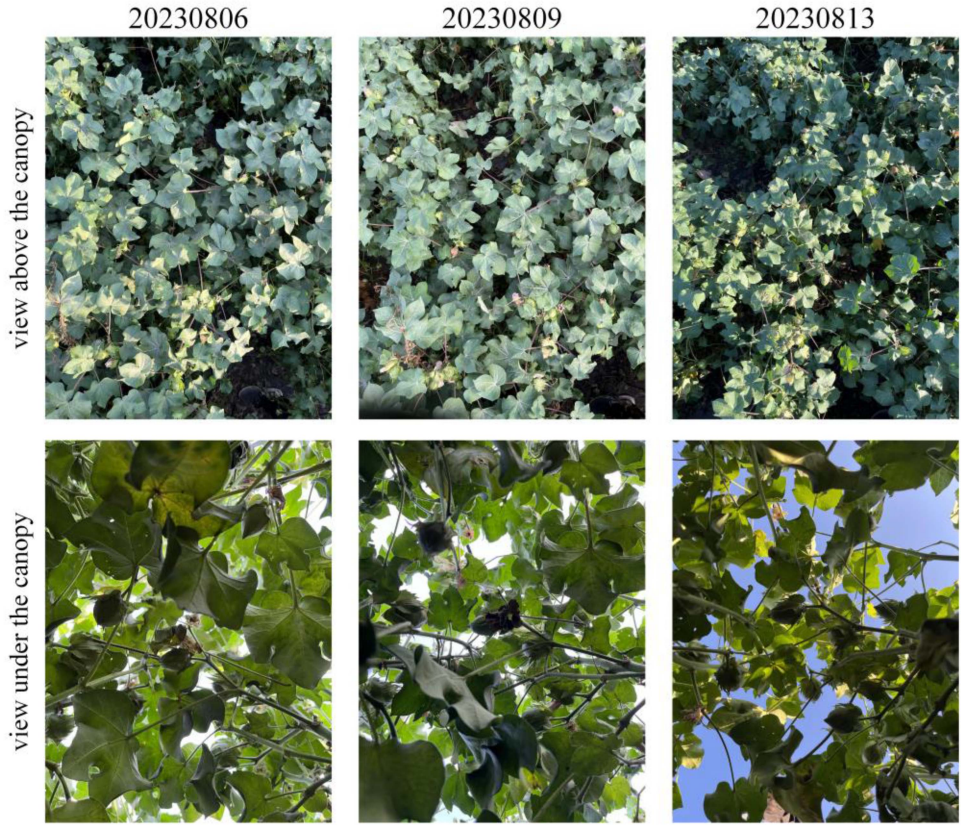

Fig. 4. View above and below the canopy of VW1 in the *T*2 period. Pictures in each column were taken on 6 August 2023, 9 August 2023, and 13 August 2023).

consequently the feasibility of this method in estimating ΦF, we conducted a linear regression analysis on both (see Fig. 6).

It was found that the relative changes caused by the retention of 7 decimal places (Round7) were not too large (see Fig. 7), and within the 15 parallel samples, the absolute value of the maximum relative change was 7.4%. Among the four types of Gaussian random noise, the one with a standard deviation of 0.01 (GS_001) caused the smallest relative change, but it still caused a change of 12.7% [see Fig. 7(f)]. With the increase of the standard deviation, the relative change in the result gradually expanded, accompanied by a gradual decline in stability. It led to large relative changes and poor stability of the results to set the standard deviation to 0.1 times the standard deviation of the parameter (GS_Std01). Similarly, setting the standard deviation as parametric standard deviation (GS_Std) caused remarkable changes in the relative importance results, with the highest relative change reaching 216.1% [see Fig. 7(b)], and the results exhibited substantial instability [see Fig. 7(c)].

In conclusion, the relative changes of results caused by various random errors indicate that retaining seven decimal places (Round7) led to relatively minor alterations among five types of random errors. Gaussian random noise with a standard deviation set at 0.01 (GS_001) resulted in small and stable relative changes. Conversely, the relative changes caused by Gaussian random noise with a standard deviation set at its own standard deviation (GS_Std) were remarkable and highly unstable. Based on the above experimental findings, it is recommended that when using the LMG model to assess the relative importance of each parameter in the SIF conceptual model, alternative parameters representing the same physical characteristics can be employed to calculate ΦF. For instance, in this study, both NIRv and FCVI serve as the representations of nonphysiological factors, exhibiting a notably high coefficient of determination in their linear regression. Thus, when NIRv was utilized for estimating fPAR $\times f_{\mathrm{esc}}$, FCVI was used for estimating ΦF, presenting a practical calculation strategy aligned with the model's principles.

IV. Discussion

A. Effects of VW on Cotton Canopy

Various vegetation parameters reflect the state of vegetation canopy in different aspects. As depicted in Fig. 3, VIs used to depict canopy structure exhibit different responses in the canopy of healthy cotton plants compared with those under varying levels of stress. Comparing the values at the end with the beginning of the experimental period, it can be found that the decrease in VW3 is much greater than that in VW4. This phenomenon occurs due to the progression of VW, which is characterized from the bottom up, with the leaves in the lower part of the canopy first turning yellow and shedding. With the aggravation of the stress, the upper leaves may also gradually fall off, resulting in sparse cotton canopy [43]. Comparing Fig. 8(b) and (d), it can be observed that VW3 in the *T*4 period exhibited

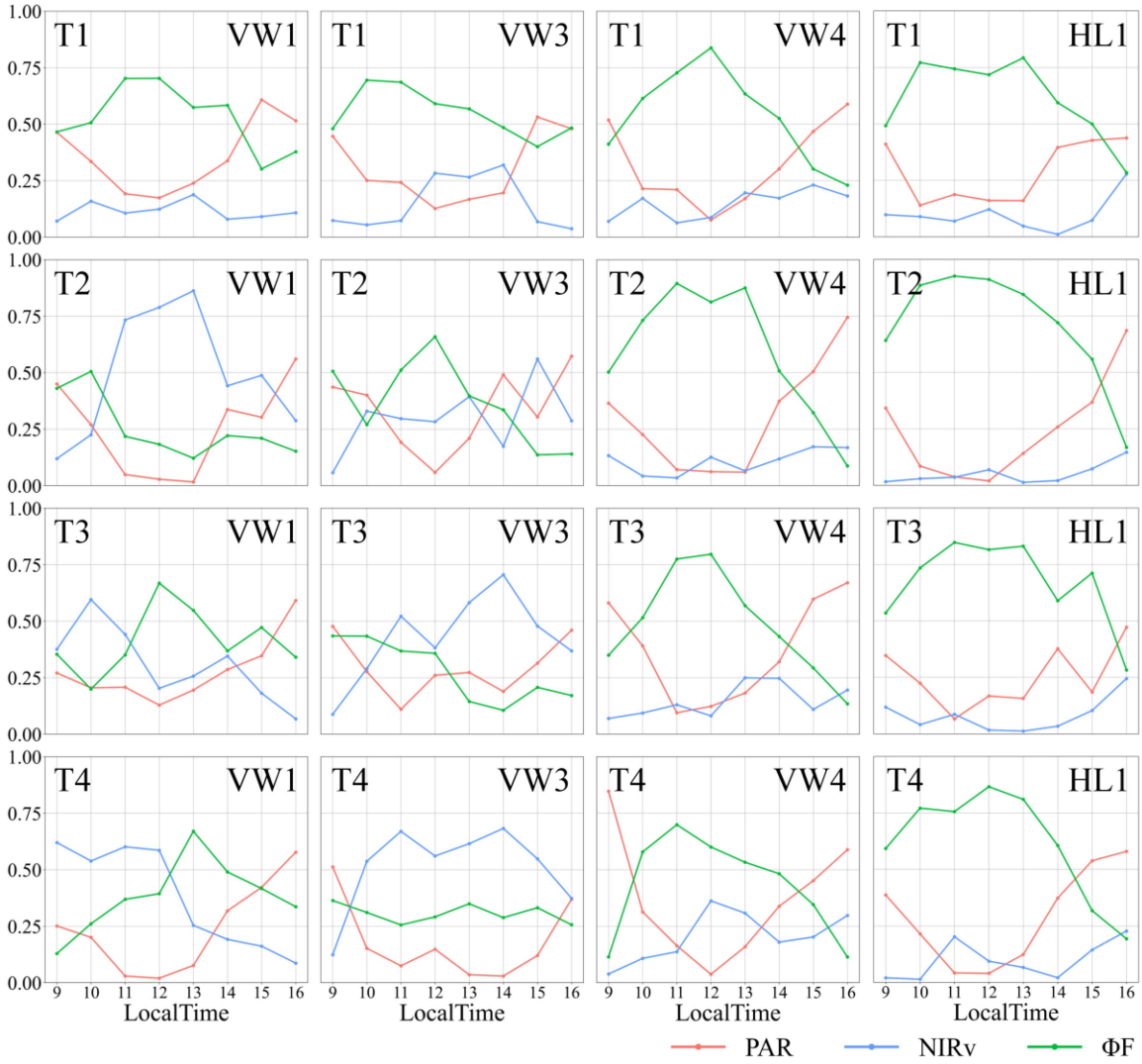

Fig. 5. Results of diurnal changes in the relative importance of each subperiod. The *x*-axis coordinates have been converted to local time. Each row corresponds to subperiods *T*1, *T*2, *T*3, and *T*4 and each column represents VW1, VW3, VW4, and HL1.

a reduction in canopy leaves and a notable increase in the proportion of sky compared with *T*1 period. Differently, VW4 showed a minor variation, which possibly indicates its lower susceptibility to VW stress than VW3, leading to a lower level of stress during the same time period compared with VW4. Leaf senescence and subsequent shedding, resulting from VW stress, initially manifest in the lower canopy leaves. However, these changes under the canopy are challenging to be detected under the vertical downlook observation mode of this experiment. RENDVI, indicating the canopy chlorophyll content, showed a declining trend across all observation points. The comparison of the RENDVI value of VW3 and VW4 in Fig. 3 revealed a more pronounced decline in VW3 than that in VW4. This finding is consistent with previous studies that conducted physical–chemical experiments on leaves exposed to various stress levels, which concluded that chlorophyll content was lower in more severely stressed leaves [6], [44], [45]. This is also evident in Fig. 8, where during the *T*4 period, leaves at the upper canopy of VW3 displayed yellowing [see Fig. 8(c) and (d)], while those of VW4 and HL1 still appeared green [see Fig. 8(g) and (h)]. This phenomenon occurs due to the accelerated yellowing of leaves at equivalent leaf ages or positions in both the upper and lower sections of cotton plants affected by VW compared with healthy counterparts. This leads to a substantial reduction in chlorophyll content, especially in severely affected cotton plants [46]. The RENDVI of VW4 and HL1 canopy exhibited a relatively small decrease, potentially attributed to the fact that, during the *T*4 period, the cotton plants had reached the late stage of their growth period, naturally leading to an overall decrease in chlorophyll in the canopy as the natural progression of cotton plant growth toward senescence. In addition, the yellowing and aging of leaves below the canopy due to VW stress in VW4 would further contribute to a decline in canopy chlorophyll content compared with HL1.

The SIF and SIF_PAR of VW3, VW4, and HL1 presented a decreasing trend from *T*1 to *T*4, with VW4 and HL1 showing a smaller decrease compared with VW3. This suggested a reduction in the photosynthetic performance of cotton plants under

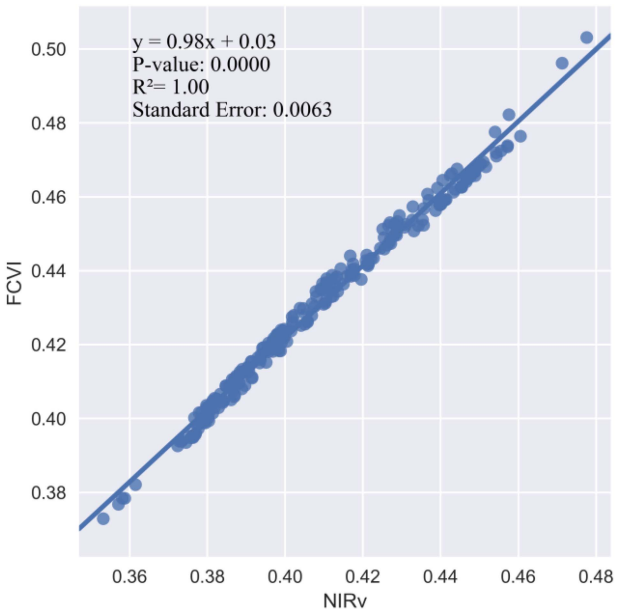

Fig. 6. Linear regression results for NIRv and FCVI.

VW stress. This observation is consistent with previous studies on leaf scale chlorophyll fluorescence [5], [27], [44], as well as existing researches on vegetation under disease stress [7], [8], [19]. Further observation revealed a slight decrease in the SIF of VW3 in $T1$–$T2$ period, with an increased amplitude of decline in $T3$–$T4$ period. Conversely, VW4 exhibited a minimal decrease throughout the whole experimental period. The above variations may stem from differences in disease tolerance among the cotton plants. Although under the same growing environment, VW4 experienced milder stress compared with VW3, with the stress degree of VW4 in $T4$ similar to that of VW3 in $T2$. This phenomenon may be attributed to the fact that, when the stress level is mild, the leaves have not been directly infected by *Verticillium dahliae*, but the physiological state of the entire cotton plant undergoes changes due to the stress. As the stress degree intensified, photosystem II (PSII) was damaged, resulting in weakened photosynthesis. With further intensification of VW stress, the chlorophyll content of the leaves decreased, and the vascular bundle of the cotton plant was blocked, hindering the transport of water and nutrients inside cotton plants, leading to a significant inhibition of the primary reaction of photosynthesis [45], [47], [48]. The fluctuation of ΦF during $T1$–$T4$, combined with the decrease of SIF_PAR, suggested that the decline of SIF during the whole period following VW stress was the outcome of both physiological and nonphysiological changes [20], [22], [25], [49], [50].

B. Dominant Drivers of the Variations of SIF Under VW Stress

It is worth noting that the diurnal variation of relative importance of each component was a composite result influenced by two factors: differences in the same time period within a day and among days within subperiod. As shown in Fig. 5, in the $T1$ period, the relative importance of PAR obtained higher values in the morning and evening, and lower values near noon. This is because the absolute value of PAR undergoes an arch-like change, exhibiting large changes in the morning and evening, and minor changes near noon in the same time interval due to the minimal variation in PAR among days within subperiod.

The results showed that the diurnal variation of each parameter's importance to SIF variations could reflect the degree of VW stress. At the early stages of VW development, the SIF variation was prominently driven by physiological factors (ΦF) for the following reasons. On the one hand, the cotton plant demonstrated a strong capacity for self-regulation of its photosynthetic processes. The rate of photosynthesis fluctuates in response to variations in light intensity, air temperature, and water conditions [51], [52], [53], [54]. On the other hand, when initially subjected to VW stress, reversible inactivation of the PSII reaction center happened and nonphotochemical quenching (NPQ) was activated as a photoprotective mechanism in protecting plants from photodamage [55], resulting in the decline of ΦF. This is similar to drought and heat stress, which induce a decline in fluorescence emission due to an increase in NPQ [20], [22], [56], [57]. This occurs in this study because VW stress causes vessel occlusion, leading to water deficiency in cotton plants [58]. As VW stress intensified, the internal physiological structure of cotton leaves was damaged [5], [47], leading to a reduced photosynthetic activity in mesophyll cells. Meanwhile, some nonphysiological impacts of VW stress on the canopy appeared from bottom to up, such as leaf chlorosis, necrosis, and finally leaf abscission [58], causing the decline of leaf chlorophyll content and leaf area at the canopy scale [8].

The effect of physiological and nonphysiological on SIF variations is closely related to the severity and type of stress. SIF variations were influenced by both physiological and nonphysiological aspects under VW stress, with the former initially greater than the latter. As VW stress intensified, the nonphysiological impacts increased and eventually surpassed the physiological effects, for the typical bottom-up damage characteristic of VW. The joint regulation of physiological and nonphysiological information was also detected in the case of water stress, which is slow and sustained, similar to VW stress. The prominent response of physiological information was detected at the early stages of water stress on sugar beet plants [20]. The importance of nonphysiological information increased to a similar value as the physiological in determining SIF variations when data were collected in a potato crop two weeks after the presence of water exclusion, for dynamic changes in leaf angular distributions in response to water stress [22]. However, the mechanism of herbicide stress is different. It can induce a rapid and well-characterized impact on the photosynthetic apparatus by inhibiting the photosynthetic electron transport from PSII to photosystem I (PSI) [59]. Therefore, the importance of physiological information to SIF variations increased rapidly and significantly within just several hours after herbicide treatment. After the early stage of treatment, it gradually decreased and eventually stabilized at values similar to those before the treatment within approximately two weeks [29]. When plants are subjected to different types of stress, they respond adaptively to these stresses by adjusting their morphology, physiology, and other means

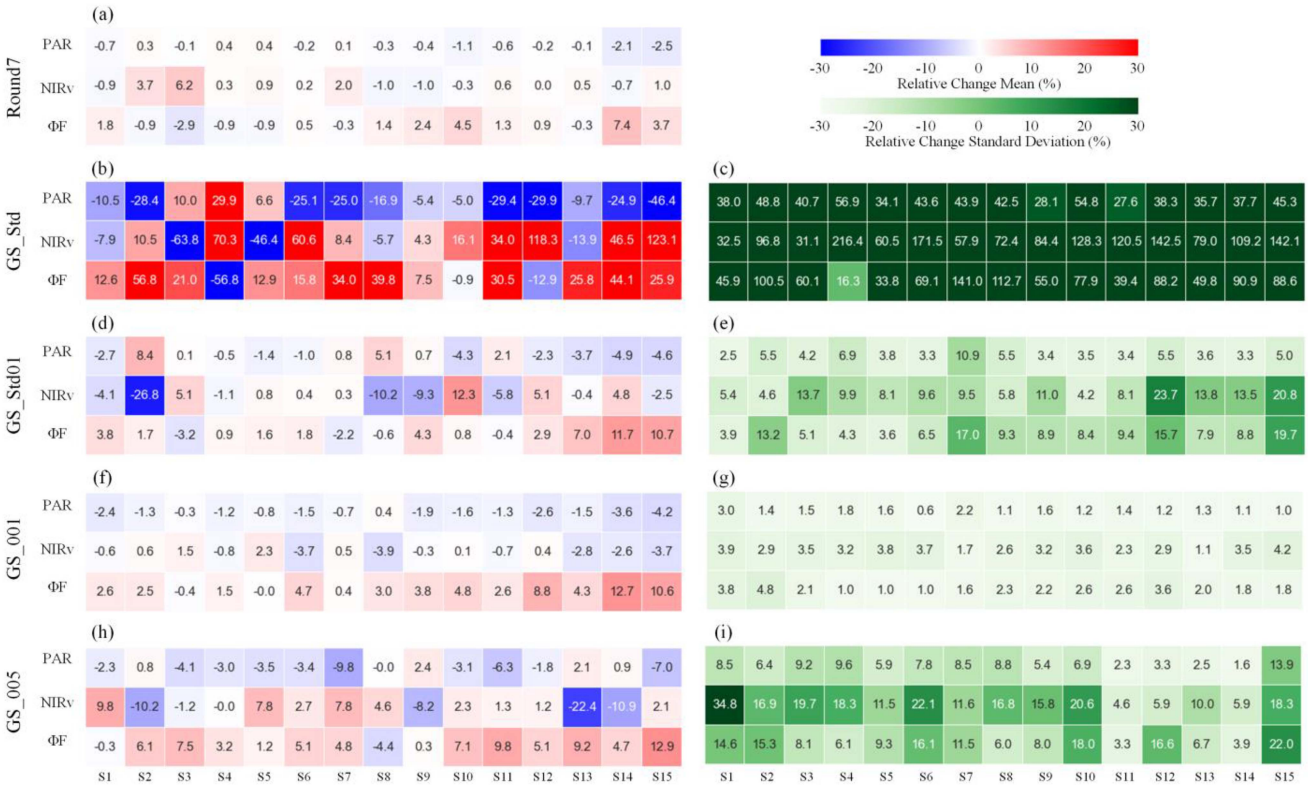

Fig. 7. Variation introduced by random error in relative importance results. *S*1–*S*15 represent 15 parallel samples, with each sample undergoing five repeated tests. Results in the left column represent the average of relative changes caused by errors and results in the right column represent the standard deviation of relative changes caused by errors.

[60], [61], [62]. Thus, when analyzing the relative importance results, it is important to deeply comprehend the mechanism of stress impact on plants.

C. Influence of Random Error on Relative Importance Results

According to Fig. 7, we found that the relative change caused by Round7 and GS_001 was relatively small among the five types of errors, but they still have the potential to alter the trend of result. If the standard deviation of Gaussian random noise was enlarged to 0.05, the relative change resulting from human error would be unacceptable and even worse when the standard deviation was further increased. Our results indicated that, although human error could make the LMG model work, it introduced uncertainty into results. It is worth noting that some errors might be introduced into data during the period of observing and processing data. During the observing period, some errors might be caused by environmental condition, such as poor weather, unstable illumination, and large solar zenith angle, which will influence the quality of observed data [63], [64]. As some research reported, variations of SIFyield (SIF/PAR/fPAR) were entirely overshadowed by the noise present in the spectral measurements and the retrieved values at the canopy scale [65]. In addition, during data processing, such as rounding retention, variations in default data accuracy across different programming languages may introduce errors in data. In order to obtain reliable and accurate results, it is important to be cautious of factors that may potentially introduce errors in the observed data.

D. Applications and Prospects

SIF has been proven as a quick and powerful tool for detecting vegetation stress. However, the observed canopy SIF is influenced by various factors during the radiative transfer process, leading to uncertainties in its direct relationship with vegetation photosynthesis. This greatly impacts the understanding and application of SIF in response to disease stress. It is of great importance to disentangle the physiological and nonphysiological components of canopy SIF to precisely depict the impact of stress on vegetation during the onset and progression of disease stress. Our results indicated that SIF variations were initially regulated by physiological information and, subsequently, by nonphysiological information as the impact of VW stress intensified, enhancing our comprehension of change process in cotton plants under VW stress. These findings are of great significance for accurately monitoring the degree of stress on cotton, as well as for the comprehensive prevention and control of cotton VW.

In future studies, it would be beneficial to incorporate more comprehensive experimental data, including photosynthesis and chlorophyll at leaf level, and structural parameters (leaf area index and leaf inclination angle distribution) at canopy level to provide more comprehensive and more intuitive insight into changes of cotton plants. More specific canopy structure data

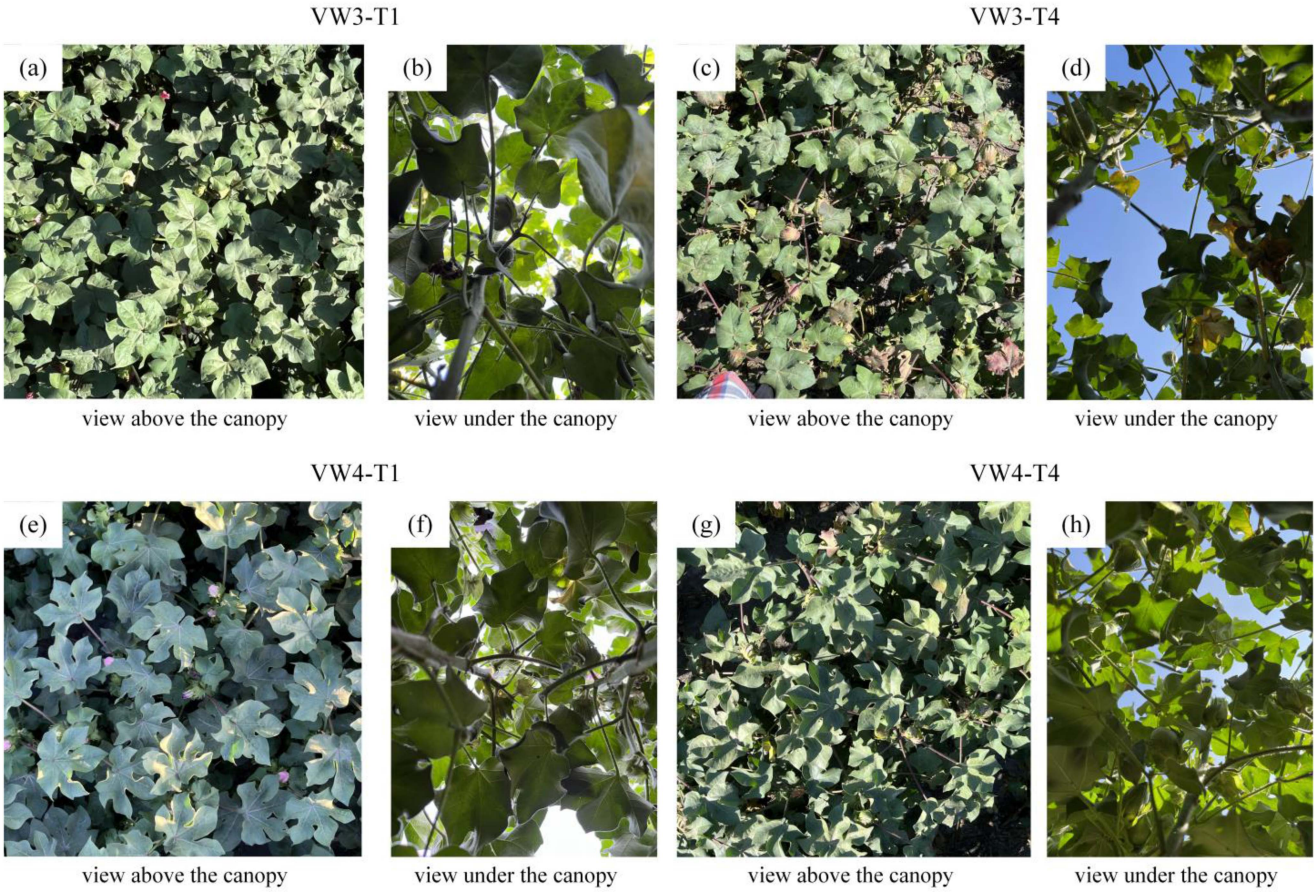

Fig. 8. View above and under the canopy of VW3 and VW4 during *T*1 and *T*4.

provide a more detailed description of fPAR and f_{esc} individually, which although is considered as the combined effect of nonphysiological information in this study. From the physical mechanism, the combination of fPAR and f_{esc} would absorb the changes in each of them. For example, the decrease in leaf area index results in a decrease in fPAR and an increase in f_{esc} [20]. Therefore, it is necessary to analyze fPAR and f_{esc} separately for better depicting nonphysiological impacts of VW stress. Furthermore, if actual measurement data are lacking or difficult to acquire, it is advisable to utilize radiative transfer model simulation results.

A number of studies have proved the capacity of SIF in estimating GPP [18], [66], [67], and it is beneficial for cotton yield estimation under VW stress to understand SIF variations better and more comprehensively. With the fast development of technology, these findings may contribute to estimating cotton yield at larger spatial scale, such as at field or county level based on the data acquired from UAV or satellite-based sensors.

V. Conclusion

In this study, we conducted continuous observation on both healthy and stressed cotton plants during the peak incidence period of VW stress. We compared and analyzed the changes in the physiological, nonphysiological factors, and SIF of the cotton canopy under different degrees of VW stress, followed by an exploration of the factors contributing to the reduction of canopy SIF. Results indicated that the regulatory role of SIF components in its variation varied under different levels of VW stress, reflecting the severity of VW. At the early stages of VW development, the changes in canopy SIF were significantly affected by physiological factors with maximum contribution close to 0.7, and the diurnal pattern exhibited an arch shape. As the VW severity increased, the contribution of physiological factors declined greatly, with the maximum contribution decreasing by 47.7%, and nonphysiological factors played a more substantial role in the changes of canopy SIF. In addition, the arch shape of physiological factors' diurnal change pattern was gradually destroyed, with the diurnal variation amplitude declining by 63.4%. Besides, we proposed a practical strategy for estimating ΦF when calculating the relative importance of parameters to SIF variations using the LMG model. This study helps to further understand the impact of VW stress on cotton plants, enhancing our comprehension of each SIF component's contribution to SIF variations in cotton plants under varying VW stress severity, thereby contributing to the accurate diagnosis of VW stress severity.

APPENDIX

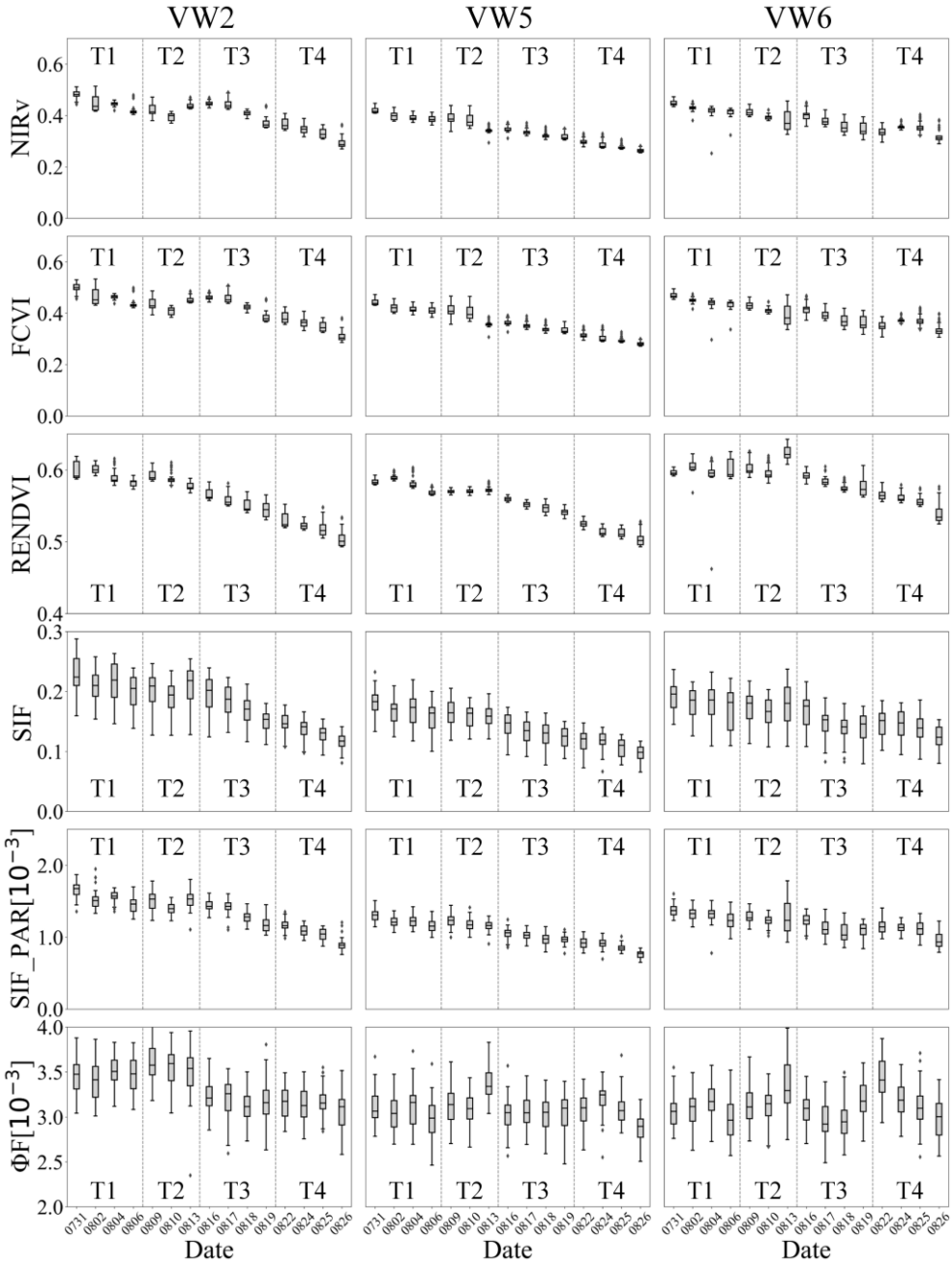

Fig. 9. Daily variations in nonphysiological factors (NIRv, FCVI, and RENDVI), SIF, SIF_PAR, and physiological factors (ΦF) during the experimental period. Each column represents VW2, VW5, and VW6.

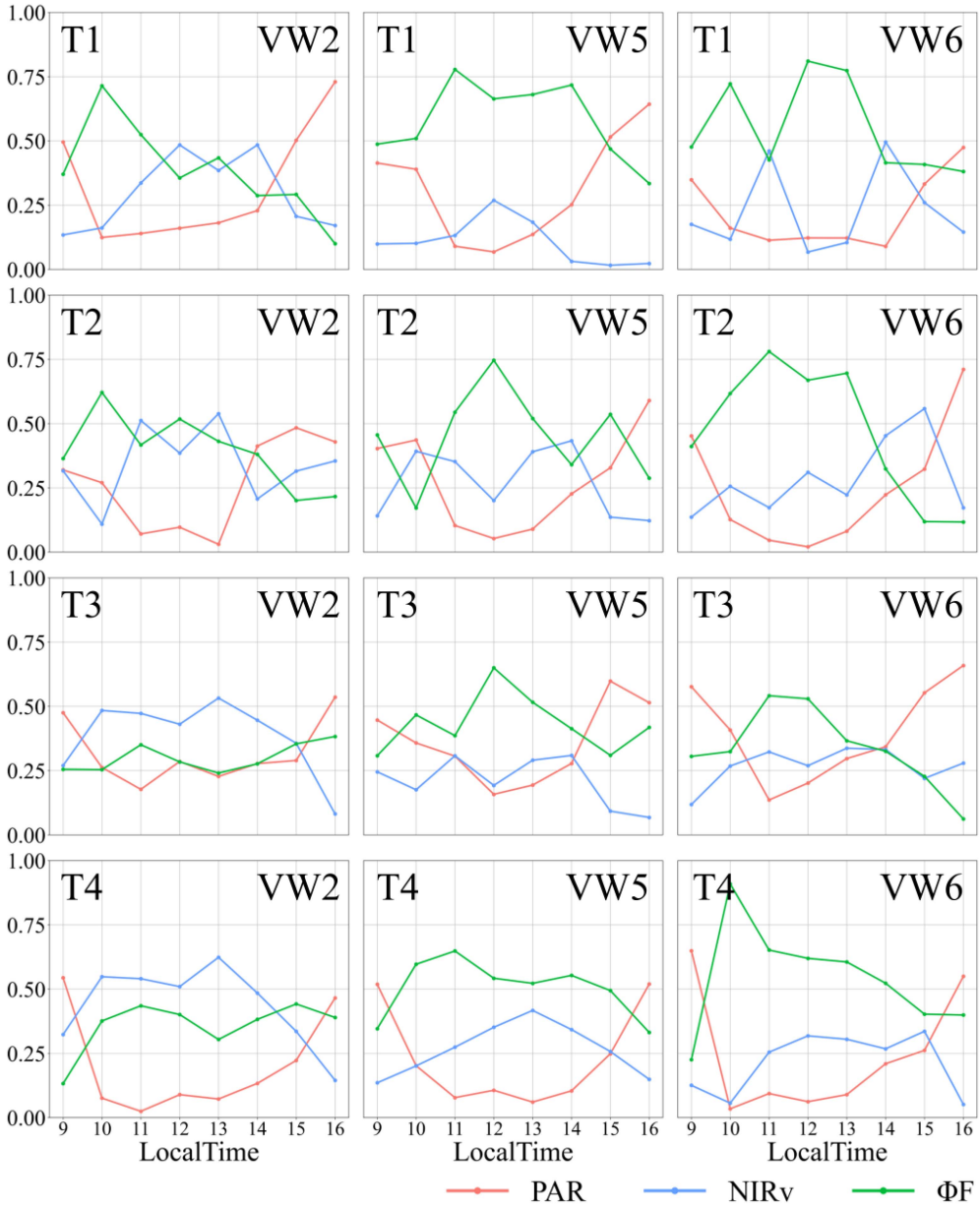

Fig. 10. Results of diurnal changes in the relative importance of each subperiod. The *x*-axis coordinates have been converted to local time in Xinjiang. Each row corresponds to subperiods *T*1, *T*2, *T*3, and *T*4 and each column represents VW2, VW5, and VW6.

ACKNOWLEDGMENT

The authors would like to thank the Director C. You from the Shihezi Institute of Agricultural Sciences for the support in coordinating the experimental field.

REFERENCES

[1] R. Song, J. Li, C. Xie, W. Jian, and X. Yang, "An overview of the molecular genetics of plant resistance to the verticillium wilt pathogen verticillium dahliae," *Int. J. Mol. Sci.*, vol. 21, no. 3, Feb. 2020, Art. no. 1120, doi: 10.3390/ijms21031120.

[2] D.-D. Zhang et al., "Population genomics demystifies the defoliation phenotype in the plant pathogen verticillium dahliae," *New Phytologist*, vol. 222, no. 2, pp. 1012–1029, 2019, doi: 10.1111/nph.15672.

[3] J. S. Gerik and O. C. Huisman, "Study of field-grown cotton roots infected with Verticillium dahliae using an immunoenzymatic staining technique," *Phytopathology*, vol. 78, no. 9, pp. 1174–1178, 1988, doi: 10.1094/Phyto-78-1174.

[4] Z. Lu et al., "Intelligent identification on cotton verticillium wilt based on spectral and image feature fusion," *Plant Methods*, vol. 19, no. 1, Jul. 2023, Art. no. 75, doi: 10.1186/s13007-023-01056-4.

[5] M. Yang et al., "Method for early diagnosis of verticillium wilt in cotton based on chlorophyll fluorescence and hyperspectral technology," *Comput. Electron. Agriculture*, vol. 216, Jan. 2024, Art. no. 108497, doi: 10.1016/j.compag.2023.108497.

[6] M. Yang et al., "Early monitoring of cotton verticillium wilt by leaf multiple 'symptom' characteristics," *Remote Sens.*, vol. 14, no. 20, Jan. 2022, Art. no. 5241, doi: 10.3390/rs14205241.

[7] R. Calderón, J. A. Navas-Cortés, and P. J. Zarco-Tejada, "Early detection and quantification of verticillium wilt in olive using hyperspectral and thermal imagery over large areas," *Remote Sens.*, vol. 7, no. 5, pp. 5584–5610, May 2015, doi: 10.3390/rs70505584.

[8] R. Calderón, J. A. Navas-Cortés, C. Lucena, and P. J. Zarco-Tejada, "High-resolution airborne hyperspectral and thermal imagery for early detection of verticillium wilt of olive using fluorescence, temperature and narrow-band spectral indices," *Remote Sens. Environ.*, vol. 139, pp. 231–245, Dec. 2013, doi: 10.1016/j.rse.2013.07.031.

[9] B. Chen et al., "Spectrum characteristics of cotton canopy infected with verticillium wilt and applications," *Agriculture Sci. China*, vol. 7, no. 5, pp. 561–569, May 2008, doi: 10.1016/S1671-2927(08)60053-X.

[10] X. Kang, C. Huang, L. Zhang, M. Yang, Z. Zhang, and X. Lyu, "Assessing the severity of cotton verticillium wilt disease from in situ canopy images and spectra using convolutional neural networks," *Crop J.*, vol. 11, pp. 933–940, Jun. 2023, doi: 10.1016/j.cj.2022.12.002.

[11] N. Zhang et al., "Detection of cotton verticillium wilt disease severity based on hyperspectrum and GWO-SVM," *Remote Sens.*, vol. 15, no. 13, Jan. 2023, Art. no. 3373, doi: 10.3390/rs15133373.

[12] N. Zhang et al., "Progress and prospects of hyperspectral remote sensing technology for crop diseases and pests," *Nat. Remote Sens. Bull.*, vol. 25, no. 1, pp. 403–422, 2021, doi: 10.11834/jrs.20210196.

[13] L. Ji and A. J. Peters, "Assessing vegetation response to drought in the northern great plains using vegetation and drought indices," *Remote Sens. Environ.*, vol. 87, no. 1, pp. 85–98, Sep. 2003, doi: 10.1016/S0034-4257(03)00174-3.

[14] L. Liu, J. Zhao, and L. Guan, "Tracking photosynthetic injury of paraquat-treated crop using chlorophyll fluorescence from hyperspectral data," *Eur. J. Remote Sens.*, vol. 46, no. 1, pp. 459–473, Jan. 2013, doi: 10.5721/EuJRS20134627.

[15] S. N. Raji et al., "Detection of mosaic virus disease in cassava plants by sunlight-induced fluorescence imaging: A pilot study for proximal sensing," *Int. J. Remote Sens.*, vol. 36, no. 11, pp. 2880–2897, Jun. 2015, doi: 10.1080/01431161.2015.1049382.

[16] Y. K. Tischler, E. Thiessen, and E. Hartung, "Early optical detection of infection with brown rust in winter wheat by chlorophyll fluorescence excitation spectra," *Comput. Electron. Agriculture*, vol. 146, pp. 77–85, 2018, doi: 10.1016/j.compag.2018.01.026.

[17] Y. Zhang, W. Huang, J. Wang, L. Liu, Z. Ma, and F. Li, "Chlorophyll fluorescence sensing to detect stripe rust in wheat (Triticum aestivum L.) fields based on Fraunhofer lines," *Scientia Agricultura Sinica*, vol. 40, no. 1, pp. 78–83, 2007.

[18] L. Guanter et al., "Global and time-resolved monitoring of crop photosynthesis with chlorophyll fluorescence," *PNAS*, vol. 111, no. 14, pp. E1327–E1333, Mar. 2014, doi: 10.1073/pnas.1320008111.

[19] P. J. Zarco-Tejada et al., "Previsual symptoms of Xylella fastidiosa infection revealed in spectral plant-trait alterations," *Nature Plants*, vol. 4, no. 7, pp. 432–439, Jul. 2018, doi: 10.1038/s41477-018-0189-7.

[20] N. Wang, P. Yang, J. G. P. W. Clevers, S. Wieneke, and L. Kooistra, "Decoupling physiological and non-physiological responses of sugar beet to water stress from sun-induced chlorophyll fluorescence," *Remote Sens. Environ.*, vol. 286, Mar. 2023, Art. no. 113445, doi: 10.1016/j.rse.2022.113445.

[21] P. J. Zarco-Tejada, V. González-Dugo, and J. A. J. Berni, "Fluorescence, temperature and narrow-band indices acquired from a UAV platform for water stress detection using a micro-hyperspectral imager and a thermal camera," *Remote Sens. Environ.*, vol. 117, pp. 322–337, Feb. 2012, doi: 10.1016/j.rse.2011.10.007.

[22] S. Xu et al., "Structural and photosynthetic dynamics mediate the response of SIF to water stress in a potato crop," *Remote Sens. Environ.*, vol. 263, Sep. 2021, Art. no. 112555, doi: 10.1016/j.rse.2021.112555.

[23] A. Damm et al., "Remote sensing of sun-induced fluorescence to improve modeling of diurnal courses of gross primary production (GPP)," *Glob. Change Biol.*, vol. 16, no. 1, pp. 171–186, 2010, doi: 10.1111/j.1365-2486.2009.01908.x.

[24] P. Zarco-Tejada, "Development of a vegetation fluorescence canopy model," Eur. Space Agency, Tech. Rep. 16365/02/NL/FF, Paris, France, 2005.

[25] B. Dechant et al., "Canopy structure explains the relationship between photosynthesis and sun-induced chlorophyll fluorescence in crops," *Remote Sens. Environ.*, vol. 241, May 2020, Art. no. 111733, doi: 10.1016/j.rse.2020.111733.

[26] J. L. Monteith, "Solar radiation and productivity in tropical ecosystems," *J. Appl. Ecol.*, vol. 9, no. 3, pp. 747–766, 1972, doi: 10.2307/2401901.

[27] A. G. Ayele, T. A. Wheeler, and J. K. Dever, "Impacts of verticillium wilt on photosynthesis rate, lint production, and fiber quality of greenhouse-grown cotton (Gossypium Hirsutum)," *Plants*, vol. 9, no. 7, Jul. 2020, Art. no. 857, doi: 10.3390/plants9070857.

[28] U. Grömping, "Estimators of relative importance in linear regression based on variance decomposition," *Amer. Statist.*, vol. 61, no. 2, pp. 139–147, 2007, doi: 10.1198/000313007X188252.

[29] L. Wu, X. Zhang, M. Rossini, Y. Wu, Z. Zhang, and Y. Zhang, "Physiological dynamics dominate the response of canopy far-red solar-induced fluorescence to herbicide treatment," *Agricultural Forest Meteorol.*, vol. 323, Aug. 2022, Art. no. 109063, doi: 10.1016/j.agrformet.2022.109063.

[30] G. Miao et al., "Varying contributions of drivers to the relationship between canopy photosynthesis and far-red sun-induced fluorescence for two maize sites at different temporal scales," *J. Geophysical Res., Biogeosci.*, vol. 125, no. 2, 2020, Art. no. e2019JG005051, doi: 10.1029/2019JG005051.

[31] S. W. Maier, K. P. Günther, and M. Stellmes, "Sun-induced fluorescence: A new tool for precision farming," in *Digital Imaging and Spectral Techniques: Applications to Precision Agriculture and Crop Physiology*. Hoboken, NJ, USA: Wiley, 2004, pp. 207–222, doi: 10.2134/asaspecpub66.c16.

[32] Y. Zeng, G. Badgley, B. Dechant, Y. Ryu, M. Chen, and J. A. Berry, "A practical approach for estimating the escape ratio of near-infrared solar-induced chlorophyll fluorescence," *Remote Sens. Environ.*, vol. 232, Oct. 2019, Art. no. 111209, doi: 10.1016/j.rse.2019.05.028.

[33] G. Badgley, C. B. Field, and J. A. Berry, "Canopy near-infrared reflectance and terrestrial photosynthesis," *Sci. Adv.*, vol. 3, no. 3, Mar. 2017, Art. no. e1602244, doi: 10.1126/sciadv.1602244.

[34] P. Yang, C. van der Tol, P. K. E. Campbell, and E. M. Middleton, "Fluorescence correction vegetation index (FCVI): A physically based reflectance index to separate physiological and non-physiological information in far-red sun-induced chlorophyll fluorescence," *Remote Sens. Environ.*, vol. 240, Apr. 2020, Art. no. 111676, doi: 10.1016/j.rse.2020.111676.

[35] P. Yang, X. Liu, Z. Liu, C. van der Tol, and L. Liu, "The roles of radiative, structural and physiological information of sun-induced chlorophyll fluorescence in predicting gross primary production of a corn crop at various temporal scales," *Agricultural Forest Meteorol.*, vol. 342, Nov. 2023, Art. no. 109720, doi: 10.1016/j.agrformet.2023.109720.

[36] A. Gitelson and M. N. Merzlyak, "Quantitative estimation of chlorophyll-a using reflectance spectra: Experiments with autumn chestnut and maple leaves," *J. Photochem. Photobiol. B*, vol. 22, no. 3, pp. 247–252, Mar. 1994, doi: 10.1016/1011-1344(93)06963-4.

[37] U. Groemping, "Relative importance for linear regression in R: The package relaimpo," *J. Statist. Softw.*, vol. 17, pp. 1–27, 2007, doi: 10.18637/jss.v017.i01.

[38] S. Han et al., "Using high-frequency PAR measurements to assess the quality of the SIF derived from continuous field observations," *Remote Sens.*, vol. 14, no. 9, Jan. 2022, Art. no. 2083, doi: 10.3390/rs14092083.

[39] L. Wang, Z. Huo, L. Zhang, Y. Jiang, J. Xiao, and X. Lu, "Effects of climate change on the occurrence of crop diseases in China," *Chin. J. Ecol.*, vol. 31, no. 7, pp. 1673–1684, Jul. 2012.

[40] X. Li, Y. Zhang, C. Ding, W. Xu, and X. Wang, "Temporal patterns of cotton fusarium and verticillium wilt in Jiangsu coastal areas of China," *Sci. Rep.*, vol. 7, no. 1, Oct. 2017, Art. no. 12581, doi: 10.1038/s41598-017-12985-1.

[41] C. Ma, "Research on cotton fusarium and verticillium wilt," China Agriculture Press, Beijing, China, 2007. [Online]. Available: https://books.google.com/books?id=eYcbQwAACAAJ

[42] F. Xu, L. Yang, J. Zhang, X. Guo, X. Zhang, and G. Li, "Effect of temperature on conidial germination, mycelial growth and aggressiveness of the defoliating and nondefoliating pathotypes of verticillium dahliae from cotton in China," *Phytoparasitica*, vol. 40, no. 4, pp. 319–327, Sep. 2012, doi: 10.1007/s12600-012-0232-6.

[43] C. H. Beckman, *The Nature of Wilt Diseases of Plants*, 1987. Accessed: Dec. 10, 2023. [Online]. Available: https://www.cabdirect.org/cabdirect/abstract/19932330042

[44] X. Zhang, Y. Li, K. Yu, Y. Huo, Y. Wang, and B. Chen, "Mechanism of verticillium wilt stress affecting photosynthetic characteristics and chlorophyll fluorescence characteristics of cotton seedlings," *Cotton Sci.*, vol. 30, no. 2, pp. 136–144, 2018.

[45] B. Chen, K. Wang, S. Li, X. Jin, J. Chen, and D. Zhang, "The effects of disease stress on spectra reflectance and chlorophyll fluorescence characteristics of cotton leaves," *Trans. CSAE*, vol. 27, no. 9, pp. 86–93, 2011.

[46] X. Pan, S. Deng, and X. Cui, "Effects of verticillium wilt of cotton on leaf photosynthesis efficiency and cotton plant growth," *Acta Entomologica Sinica*, vol. 6, no. S1, pp. 64–68, 1994.

[47] B. Chen et al., "Effects of verticillum wilt on leaf microstructure, photosynthesis of cotton," *Cotton Sci.*, vol. 29, no. 6, pp. 570–578, 2017.

[48] S. H. Temple, J. DeVay, and L. L. Forrester, "Temperature effects upon development and pathogenicity of defoliating and nondefoliating pathotypes of verticillium dahliae in leaves of cotton plants," *Phytopathology*, vol. 63, pp. 953–958, 1973, doi: 10.1094/Phyto-63-953.

[49] C. van der Tol, J. A. Berry, P. K. E. Campbell, and U. Rascher, "Models of fluorescence and photosynthesis for interpreting measurements of solar-induced chlorophyll fluorescence," *J. Geophysical Res. Biogeosci.*, vol. 119, no. 12, pp. 2312–2327, 2014, doi: 10.1002/2014JG002713.

[50] Y. Hwang, J. Kim, and Y. Ryu, "Canopy structural changes explain reductions in canopy-level solar induced chlorophyll fluorescence in prunus yedoensis seedlings under a drought stress condition," *Remote Sens. Environ.*, vol. 296, Oct. 2023, Art. no. 113733, doi: 10.1016/j.rse.2023.113733.
[51] A. J. Mohotti and D. W. Lawlor, "Diurnal variation of photosynthesis and photoinhibition in tea: Effects of irradiance and nitrogen supply during growth in the field," *J. Exp. Botany*, vol. 53, no. 367, pp. 313–322, Feb. 2002, doi: 10.1093/jexbot/53.367.313.
[52] Y. Miao, Y. Cai, H. Wu, and D. Wang, "Diurnal and seasonal variations in the photosynthetic characteristics and the gas exchange simulations of two rice cultivars grown at ambient and elevated CO_2," *Front. Plant Sci.*, vol. 12, 2021, Art. no. 25460, doi: 10.3389/fpls.2021.651606.
[53] R. Shimada and K. Takahashi, "Diurnal and seasonal variations in photosynthetic rates of dwarf pine pinus pumila at the treeline in central Japan," *Arctic, Antarctic, Alpine Res.*, vol. 54, no. 1, pp. 1–12, Dec. 2022, doi: 10.1080/15230430.2021.2022995.
[54] E. L. Singsaas, D. R. Ort, and E. H. DeLucia, "Diurnal regulation of photosynthesis in understory saplings," *New Phytologist*, vol. 145, no. 1, pp. 39–49, 2000, doi: 10.1046/j.1469-8137.2000.00556.x.
[55] A. V. Ruban, "Nonphotochemical chlorophyll fluorescence quenching: Mechanism and effectiveness in protecting plants from photodamage," *Plant Physiol.*, vol. 170, no. 4, pp. 1903–1916, Apr. 2016, doi: 10.1104/pp.15.01935.
[56] A. Ač, Z. Malenovský, J. Olejníčková, A. Gallé, U. Rascher, and G. Mohammed, "Meta-analysis assessing potential of steady-state chlorophyll fluorescence for remote sensing detection of plant water, temperature and nitrogen stress," *Remote Sens. Environ.*, vol. 168, pp. 420–436, Oct. 2015, doi: 10.1016/j.rse.2015.07.022.
[57] L. Song et al., "Satellite sun-induced chlorophyll fluorescence detects early response of winter wheat to heat stress in the Indian Indo-Gangetic plains," *Glob. Change Biol.*, vol. 24, no. 9, pp. 4023–4037, 2018, doi: 10.1111/gcb.14302.
[58] E. F. Fradin and B. P. H. J. Thomma, "Physiology and molecular aspects of Verticillium wilt diseases caused by V. Dahliae and V. Albo-atrum," *Mol. Plant Pathol.*, vol. 7, no. 2, pp. 71–86, Mar. 2006, doi: 10.1111/j.1364-3703.2006.00323.x.
[59] M. Celesti et al., "Exploring the physiological information of sun-induced chlorophyll fluorescence through radiative transfer model inversion," *Remote Sens. Environ.*, vol. 215, pp. 97–108, Sep. 2018, doi: 10.1016/j.rse.2018.05.013.
[60] C. Zhao, H. Zhang, C. Song, J. - K. Zhu, and S. Shabala, "Mechanisms of plant responses and adaptation to soil salinity," *Innovation*, vol. 1, no. 1, May 2020, Art. no. 100017, doi: 10.1016/j.xinn.2020.100017.
[61] T. C. Hsiao, "Plant responses to water stress," *Annu. Rev. Plant Biol.*, vol. 24, no. 1, pp. 519–570, 1973, doi: 10.1146/annurev.pp.24.060173.002511.
[62] D.-D. Zhang, X.-F. Dai, S. J. Klosterman, K. V. Subbarao, and J.-Y. Chen, "The secretome of verticillium dahliae in collusion with plant defence responses modulates Verticillium wilt symptoms," *Biol. Rev. Cambridge Philos. Soc.*, vol. 97, no. 5, pp. 1810–1822, Oct. 2022, doi: 10.1111/brv.12863.
[63] S. Cogliati et al., "Continuous and long-term measurements of reflectance and sun-induced chlorophyll fluorescence by using novel automated field spectroscopy systems," *Remote Sens. Environ.*, vol. 164, pp. 270–281, Jul. 2015, doi: 10.1016/j.rse.2015.03.027.
[64] D. Zhao et al., "Temporal resolution of vegetation indices and solar-induced chlorophyll fluorescence data affects the accuracy of vegetation phenology estimation: A study using in-situ measurements," *Ecol. Indicators*, vol. 136, Mar. 2022, Art. no. 108673, doi: 10.1016/j.ecolind.2022.108673.
[65] X. Liu et al., "Modelling the influence of incident radiation on the SIF-based GPP estimation for maize," *Agricultural Forest Meteorol.*, vol. 307, Sep. 2021, Art. no. 108522, doi: 10.1016/j.agrformet.2021.108522.
[66] C. Frankenberg et al., "New global observations of the terrestrial carbon cycle from GOSAT: Patterns of plant fluorescence with gross primary productivity," *Geophysical Res. Lett.*, vol. 38, no. 17, 2011, Art. no. L17706, doi: 10.1029/2011GL048738.
[67] J. D. Wood, T. J. Griffis, J. M. Baker, C. Frankenberg, M. Verma, and K. Yuen, "Multiscale analyses of solar-induced florescence and gross primary production," *Geophysical Res. Lett.*, vol. 44, no. 1, pp. 533–541, 2017, doi: 10.1002/2016GL070775.

Junru Zhou received the B.S. degree in geoinformation science and technology from Zhejiang University, Hangzhou, China, in 2021. He is currently working toward the M.S. degree in cartography and geographic information system with Aerospace Information Research Institute, Chinese Academy of Sciences, Beijing, China.

His research interests include hyperspectral remote sensing and vegetation disease monitoring.

Changping Huang received the B.S. degree in land resources management from Southwest University, Chongqing, China, in 2008, and the Ph.D. degree in cartography and geographical information systems from the Institute of Remote Sensing and Digital Earth, Chinese Academy of Sciences (CAS), Beijing, China, in 2014.

He is currently a Fulltime Professor and the Deputy Director of the National Engineering Laboratory for Satellite Remote Sensing Applications, Aerospace Information Research Institute, CAS. His major research interests include hyperspectral remote sensing and smart agriculture.

Yaohui Gui received the B.M. degree in land resources management and finance from Southwest University, Chongqing, China, in 2022. He is currently working toward the M.S. degree in cartography and geographic information system with the National Engineering Laboratory for Satellite Remote Sensing Applications, Aerospace Information Research Institute, Chinese Academy of Sciences, Beijing, China.

His research interest is related to hyperspectral remote sensing of vegetation diseases.

Mi Yang received the B.S.A. degree in agronomy from Shihezi University, Shihezi, China, in 2020. He is currently working toward the Ph.D. degree major in crop science with Xinjiang Production and Construction Crops Oasis Eco-Agriculture Key Laboratory, College of Agriculture, Shihezi University, Shihezi, China.

His research interest is related to hyperspectral remote sensing of vegetation diseases.

Ze Zhang received the B.S.A. degree in forestry, the M.S.A. degree in plant nutrition, and the Ph.D. degree in crop cultivation and farming systems from Shihezi University, Shihezi, China, in 2008, 2011, and 2015, respectively.

He is currently the Director of the Department of Smart Agriculture and an Associate Professor with the College of Agriculture, Shihezi University. His research interests mainly focus on smart agriculture and agricultural remote sensing.

Wenjiang Huang received the Ph.D. degree in cartography and geographical information systems from Beijing Normal University, Beijing, China, in 2005.

He is currently a Fulltime Professor with Aerospace Information Research Institute, Chinese Academy of Sciences, Beijing, China. His major research interests include quantitative remote sensing for vegetation and vegetation pest and disease monitoring. He has authored or coauthored more than 250 SCI journal papers focused on remote sensing for vegetation biophysical and biochemical variables inversion and pest and disease monitoring by remote sensing.

Lifu Zhang (Senior Member, IEEE) received the B.E. degree in photogrammetry and remote sensing from the Department of Airborne Photogrammetry and Remote Sensing, Wuhan Technical University of Surveying and Mapping, Wuhan, China, in 1992, the M.E. degree in photogrammetry and remote sensing from the State Key Laboratory of Information Engineering in Surveying, Mapping, and Remote Sensing, Wuhan Technical University of Surveying and Mapping, Wuhan, China, in 2000, and the Ph.D. degree in photogrammetry and remote sensing from the State Key Laboratory of Information Engineering in Surveying, Mapping, and Remote Sensing, Wuhan University, Wuhan, China, in 2005.

He is currently a Fulltime Professor and the Dean of Hyperspectral Remote Sensing Division, Aerospace Information Research Institute, Chinese Academy of Sciences, Beijing, China. His research interests include hyperspectral remote sensing and imaging spectrometer system development and its applications.

Dr. Zhang is a member of the International Society for Optical Engineering (SPIE), the Academy of Space Science of China, and the Chinese National Committee of the International Society for Digital Earth. He is also the Vice-Chairperson of Hyperspectral Earth Observation Committee, CNISDE, and a Standing Committeeman of the Expert Committee of the China Association of Remote Sensing Applications.

Qingxi Tong received the B.S. degree in agrometeorology from Odessa Hydrometeorological Institute, Odessa, Ukraine, in 1961.

He has been engaged in the study of the development and application of remote sensing since the beginning of 1970. He is currently the Chief Scientist in a Cooperation Project of the National Remote Sensing Center of China and Surrey Satellite Technology Ltd. (SSTL), Guildford, U.K., for the development of a small satellite. As a result, a high-performance small satellite named "Beijing1" has been launched and successfully operated. He is one of the Principal Scientists in remote sensing in China. He has made outstanding contributions in the development of remote sensing technology and applications, particularly in the development of airborne remote sensing systems and in the study of remote sensing spectral properties of Earth resources and environments.

Prof. Tong was elected as a member of the Chinese Academy of Sciences and an Academician of the International Eurasian Academy of Sciences in 1997. He was a recipient of the National Prizes for Progress of Science and Technology and the CAS Prize for Progress of Science and Technology many times due to his achievements, and the Achievement for International Remote Sensing Science and Technology by the International Society for Optical Engineering (SPIE) in 2002.